

Research on the GPS Signal Scattering and Propagation in the Tropospheric Ducts

G.C. Lee^{#1}, L. X. Guo^{#1,2}, J.J.Sun^{#1}, and J. H.Ge^{#2}

¹ School of Science, Xidian University

²State Key Lab. of Integrated Service Networks, Xidian University
Box 274, No.2, Taibai Road, Xi'an 710071, China

Abstract— In this paper, the method of moment (MoM) is used to investigate the characteristics of the GPS (Global Positioning System) signal scattering from the rough sea surface under low grazing incidence, and then on the basis of the results, the GPS signal could be received as the initial field by the improved Discrete Mixed Fourier Transform algorithm (DMFT) method to study the propagation characteristics in the tropo-spheric ducts. The advantages of MoM are shown the validity in computing the EM scattering at low grazing incident angle and also shown by the comparison of the Bistatic Scattering Coefficient (BSC) with MoM and Kirchhoff Approximation (KA). Finally, the propagation properties of GPS scattering signal in the evaporation ducts with different evaporation duct heights and elevation angles of GPS are discussed by the improved discrete mixed Fourier transform with taking into account the sea surface roughness.

I. INTRODUCTION

This paper deals with works on the GPS signal propagation in the tropospheric ducts using the improved Discrete Mixed Fourier Transform algorithm (DMFT) for the parabolic equation method[1] [2]. In recent years, radio wave propagation in the troposphere has been attended extensively by many researchers, especially for the radio wave propagation in the ducting environment and its effect on radar system and electronic system. When the refractivity gradient that is less than $-157N$ -units per-kilometer will result in radio wave that refracts towards the surface of the earth with a curvature that exceeds the curvature of the earth, thus radio wave will be trapped into a thin atmospheric layer, this phenomenon is similar to that of the metal waveguides. Radio system and radar of maritime operation are greatly influenced by the existence of atmospheric ducts, it can give a rise to over-the-horizon detection and form the radar detection shadow zone.

The GPS is a space-based global navigation satellite system that provides reliable location and time information in all weather and at all times and anywhere on or near the Earth when and where there is an unobstructed line of sight to four or more GPS satellites, it is freely accessible by anyone with a GPS receiver[3~4]. The GPS satellite transmits, worked at 1575.42 MHz (L1 frequency), an unique binary pseudo-random code (C/A code) and the minimum received power specified (in L1) is -160 dBW, about -20 dB under the local thermal noise. The pseudorange is estimated through correlation between the received signal and its replica generated by the receiver. The GPS receiver demodulates L1 signals with power levels between -130 and -160 dBW (in an

optimal case) corresponding to a dynamic range of 30 dB and its antenna gain ranges from about 0 (horizon) to 10 (zenith) dB in order to eliminate some multipath effects.

Currently, methods used to study the radio wave propagation in the troposphere mainly included the Parabolic Wave Equation (PWE) [2] method, Ray Tracing approach (RTA) [1] and Mode theory[5]. The PWE method have been developed and used extensively over the past twenty years to calculate the radio wave propagation problems due to its accuracy and stability, what is more important, it can consider the influence of refractive index on radio propagation in ducting environment easily. The PWE method has been widely used to model the propagation of electromagnetic and acoustic waves through inhomogeneous media. Most applications of the PWE consider low-grazing angle or near-horizontal propagation of radar or acoustic waves. In many cases, the horizontal boundary, be it terrain, ocean surface, or ocean bottom, plays a significant role. In this paper, the method of moment (MoM) [6] is used to investigate the characteristics of the GPS (Global Positioning System) signal scattering from the rough sea surface under low grazing incidence, and then on the basis of the results, the GPS signal could be received as the initial field by the SSPE method to study the propagation characteristics in the tropo-spheric ducts.

II. NUMERIC SOLUTIONS OF THE TROPOSPHERIC DUCTS PROPAGATION

The DMFT method used to solve parabolic-type equations is popular for modeling EM wave propagation in the troposphere. Leontovich and Fock [7] were pioneers who introduced the use of the PE method for solving the EM wave propagation in the atmospheric ducts. However, this approach become famous after introduced the SSPE algorithm by Tappert[8].

A. Split-step parabolic Equation Method Solution

The standard parabolic wave equation is obtained from the two-dimensional Helmholtz equation by separation the rapidly varying phase term to obtain an amplitude factor, which varies in range which is the direction of the propagation axis. The standard parabolic wave equation is given by

$$\frac{\partial^2 u}{\partial z^2} + 2ik \cdot \frac{\partial u}{\partial x} + \kappa^2 (m^2 - 1) \cdot u = 0 \quad (1)$$

Where k is the wave number in vacuum and m is the modified refractive index, x axis is the direction of the wave propagation, z axis is the height direction.

Equation (1) can be solved by a step technique where the initial field distribution $u(0,z)$ is specified at an open boundary, the solution at $(\Delta x, z)$ is obtained as a function of the initial (incident) field and of the boundary conditions at the top and bottom of the domain. After some tedious derivation, the solution of the parabolic equation is described as follow[2].

$$u(x + \Delta x, z) = e^{ikm(x,z)\Delta x/2} F^{-1} \left\{ e^{i\sqrt{k^2 - p^2}} F \left\{ e^{ikm(x,z)\Delta x/2} u(x, z) \right\} \right\} \quad (2)$$

where p is the p -space, $p = k \sin \theta$, θ is the incident angle,

Δx is the step of x , follow the Nyquist theorem, z_{\max} and p_{\max} should satisfy $z_{\max} p_{\max} = N\pi$.

For the rough dielectric ocean surface studied in the current work, the improved Discrete Mixed Fourier Transform algorithm (DMFT) method introduced by Kuttler and Dockery (1991) is employed for the simulation of GPS propagation because it incorporates an impedance boundary into the split-step solution.

From the theory of the microwave propagation, the propagation loss includes two parts: free space propagation loss and the propagation loss caused by the absorption, scattering and diffraction. Once propagation factor F is obtained, the propagation loss [8] in dB is determined by the basic radio wave theory in the form of

$$L = L_f + 20 \lg F \quad (3)$$

where L_f and F stand for free space propagation loss and propagation factor, respectively. Here, propagation loss in the free space is given by the following formula [8]

$$L_f = 32.45 + 20 \lg f(\text{MHz}) + 20 \lg r(\text{km}) \quad (4)$$

And the propagation factor F [2] is defined as

$$F = |E/E_0| \quad (5)$$

where E is the field strength at a point, and E_0 is the field strength that would occur at that point under free space conditions. In rectangular coordinate system, propagation factor [2] can be calculated by

$$F = \sqrt{x} |u(x, z)| \quad (6)$$

x is the distance between the transmitting antenna and receiving antenna, and z is the altitude measured with respect to the mean sea surface.

B. Initial field and the boundary condition

It is well known that solving the parabolic equation is related to an initial value problem, and the field in range $x + dx$ is dependent on the field at the previous range step, so one must begin with an initial field at range zero for propagation to be filed forward. In general, the far-field antenna pattern is used to calculate the initial field distribution by FFT. In this paper the GPS signal is introduced regarded as the

initial field, and the initial field is calculated by the MoM[9] with different direct incident and reflected angles and observation distances for height mesh space interval. The geometry of the initial field[10] is depicted in Fig.1.

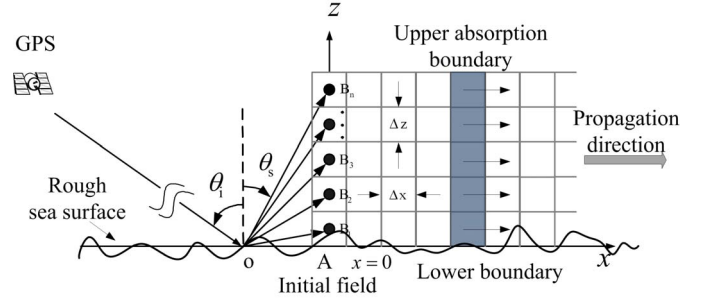


Fig.1. Initial GPS signal field with the propagation region.

The initial GPS signal field with the upper absorption region is attenuated by a Hanning window in the upper region of the implementation-domain. For the lower boundary the effective reflection coefficient is implemented through the use of FFT's in the angular spectrum domain. The incident field is used to form the source image where the 180 degree phase shift is then implemented.

For the purpose of comparing the numerical results of the bistatic scattering by KA and MoM[6], we introduce the tapered wave into the classical KA, and redefine the definition of bistatic scattering coefficient calculated by KA. In Fig. 2, the wind speed is $U = 5 \text{ m/s}$, the incidences are small incident angle $\theta_i = 20^\circ$ and large incident angle $\theta_i = 80^\circ$, respectively. From Fig. 2, it is observed that for the small incidence, σ of the results by the two methods agree with each other very well over the whole scattering region, but for the large incidence, an obvious discrepancy appearing in the non-specular direction. Therefore, the results shows that the MoM are shown the validity in computing the EM scattering at low grazing incident angle.

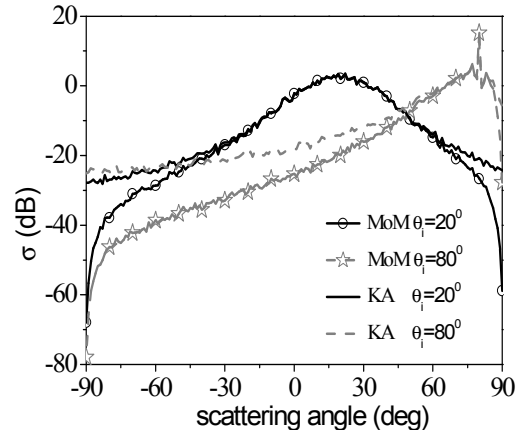
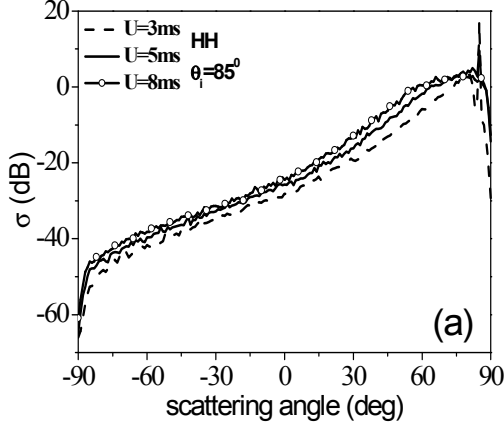


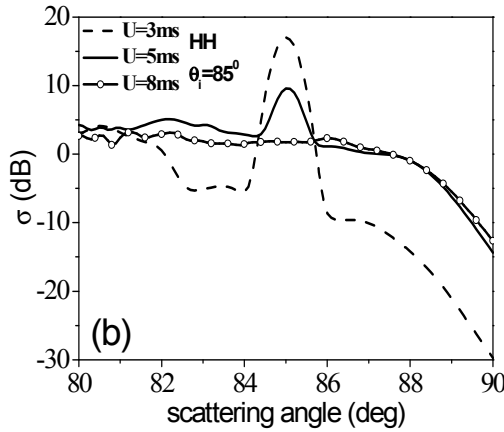
Fig.2. Comparison of σ by MoM and KA

To further examine the scattering characteristics of different wind speeds at low grazing incident angle, the bistatic scattering at incident angle $\theta_i = 85^\circ$ with different wind

speeds $U = 3$ m/s, $U = 5$ m/s and $U = 8$ m/s are presented and compared in Fig. 3(a). And σ near the specular direction $\theta_s = 80^\circ \sim 90^\circ$ is specially shown in Fig. 3(b). It is obviously seen that there is a peak in the specular direction for the smaller wind speed, which proves the point that the specular peak of the coherent wave depends on the surface roughness, we attribute this behavior to the fact that the roughness of the sea surface depends on the wind speed, the smaller wind speed, the flatter is the sea surface, leading to the obviously peak in the specular direction. Oppositely, with larger wind speed, the sea surface becomes rougher and will cause σ increasing in the direction far from the specular direction.



(a) Comparison of σ by MoM with different wind speeds



(b) Comparison of σ by MoM with different wind speeds at large scattering angles.

Fig.3. The distribution of σ for different wind speeds at low-grazing incident angle.

Fig.4 shows that the GPS scattering initial field at low grazing incident angle with different winds. The initial field obtained by calculation the Bistatic Scattering Coefficient (BSC) with MoM.

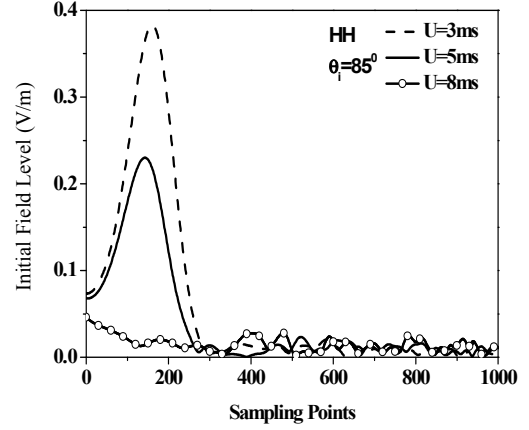


Fig.4. The GPS scattering initial field at low grazing incident angle with different winds.

C. Tropospheric duct structure

The tropospheric duct is formed by small variations in the index of refraction of the troposphere. These variations are due to the anomalous vertical gradients of temperature and humidity. The evaporation duct created by a rapid decrease in moisture immediately adjacent to the ocean surface is a nearly permanent propagation mechanism for the radar waves propagating over the ocean surface. The modified refractivity profile (M-profile) model commonly used for evaporation ducts is the log-linear Paulus-Jeske model. This model is parameterized using only the evaporation duct height (EDH) as follows:

$$M(z) = M(0) + c_0 \left(z - d \ln \frac{z + z_0}{z_0} \right) \quad (7)$$

where h is the height (m) above the mean sea level; d denotes the EDH (m); M_0 represents the modified refractivity at the sea surface, taken as 330 M-units in this paper.

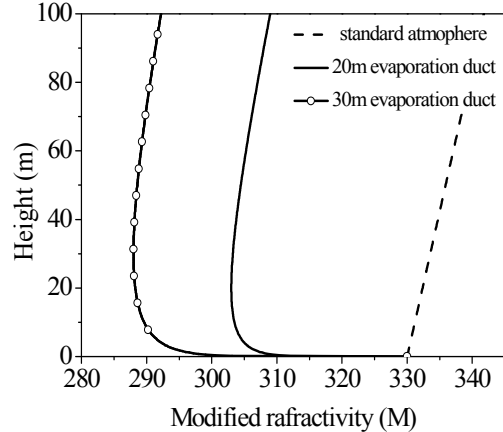


Fig.5. Modified refractivity profiles for three different atmosphere environment.

Fig.5 shows that the Modified refractivity profiles for three different atmosphere environment, $d = 0$ shows the standard atmosphere, $d = 20$ shows 20m height evaporation duct and $d = 30$ shows 30m height evaporation duct.

III. NUMERICAL RESULTS AND DISCUSSIONS

In this section, the propagation of GPS signals at different conditions are presented in Fig.6 standard atmosphere, 20m evaporation duct and 30m evaporation duct. Fig.7 gives comparison of the GPS signal propagation Loss various with range increasing and Fig.8 gives comparison of the GPS signal propagation Loss various with height increasing.

A. Analysis of the GPS signal propagation in the evaporation ducts

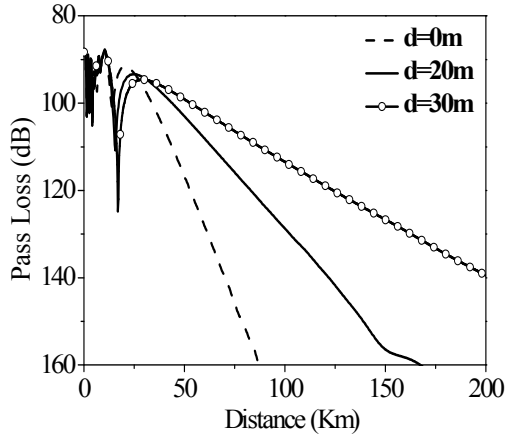


Fig.6. Comparison of the GPS signal propagation Loss various with different ducts

Fig.6 shows that the GPS signal propagation characteristics in different conditions, standard atmosphere, 20m evaporation duct and 30m evaporation duct. It is found that the great effect on the propagation characteristic in the duct condition, microwave could transform longer than the standard condition, and the higher the evaporation duct height is, the smaller the propagation loss for a fixed propagation distance will be.

B. Analysis of the GPS signal propagation loss in the tropospheric ducts with different winds

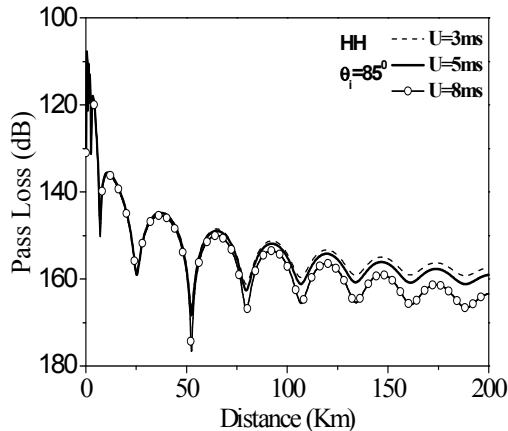


Fig.7. Comparison of the GPS signal propagation Loss various with range increasing

Fig.7 depicts the GPS signal propagation loss in the 20m evaporation duct with different winds. It is shows that all the curves of the propagation loss increase with the propagation distance increasing, and it is obviously seen that the wind do great influence on the microwave propagation in the duct, with the wind increasing, the propagation loss increased then.

Fig.8 presents the GPS signal propagation characteristics various with height increasing at range 80 Km, it is clearly seen that the wind is higher, the propagation loss is larger at 20m evaporation duct.

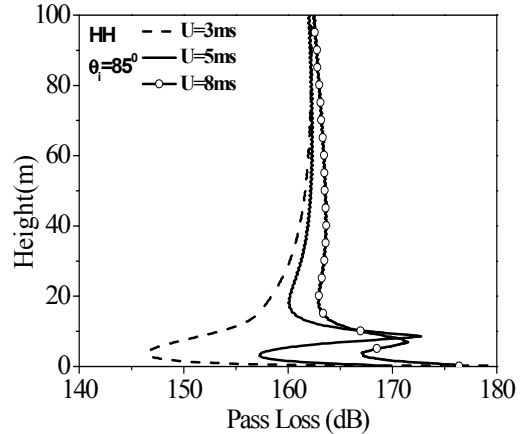


Fig.8. Comparison of the GPS signal propagation Loss various with height increasing

IV. CONCLUSION

This paper presents the GPS signal propagation characteristics in different conditions. Future investigation is the propagation characteristics in more areas, which is more important to practical application.

ACKNOWLEDGEMENT

This work was supported by the National Science Foundation for Distinguished Young Scholars of China (Grant No. 61225002), the Specialized Research Fund for the Doctoral Program of Higher Education (Grant No. 20100203110016), and the Fundamental Research Funds for the Central Universities (Grant No. K50510070001).

REFERENCES

- [1] D. E. Kerr, ed. Propagation of Short Radio Waves., London: IEE Electromagnetic Waves Series, Peter Peregrinus, 1987.
- [2] G. D. Dockery, Modeling electromagnetic wave propagation in the troposphere using the parabolic equation. IEEE Trans Ant & Prop., vol. 36, pp.1464-1470, 1988.
- [3] http://en.wikipedia.org/wiki/Global_Positioning_System
- [4] Kaplan E D. Understanding GPS Principles and Applications [M]. Artech House, Norwood,1996.
- [5] J. R. Wait, Coupled mode analysis for a nonuniform tropospheric waveguide, Radio Sci., vol.15, pp.667-673, 1980.
- [6] Ku H C, Awadallah R S, McDonald R L, and Woods N E 2006 IEEE Trans. Antennas Propag. 54 238
- [7] Leontovich M. A. and Fock V. A. Solution of the problem of propagation of electromagnetic waves along the earth's surface by method of parabolic equations. J. Phys. USSR, 1946, 10(1): 13-23.
- [8] Hardin R. H. and Tappert F. D. Applications of split-step Fourier method to the numerical solution of nonlinear and variable coefficient wave equations. SIAM Rew, 1973, 15:423.
- [9] D. E. Kerr, ed. Propagation of Short Radio Waves., London: IEE Electromagnetic Waves Series, Peter Peregrinus, 1987.
- [10] G.C.Balvedi and F.Walter, Analysis of GPS signal propagation in tropospheric ducts using numerical methods. 11th URSI Commission F Open Sysposium on radio Wave Propagation and Remote Sensing Proceedings, Rio de Janerio, RJ, Brazil, 2007.